A computer-assisted Faulted Phase Selection Algorithm for dealing with the effects of Renewable Resources in Smart grids.

Maria Teresa Villen[1]*, Maria Paz Comech[2], Eduardo Martinez[1], Roberto Matute[1], M.A. Oliván[1], Anibal Prada[1] and Jose Saldana[1]
[1] Infrastructure of Electric Grids Group, CIRCE Research Centre, Zaragoza, Spain
[2] Instituto Universitario de Investigación CIRCE, Fundación CIRCE—Universidad de Zaragoza, Zaragoza, Spain
*mtvillen@fcirce.es

Abstract

The increase in renewable generation in the grid has brought new challenges for the protection systems currently installed in the distribution and transmission network. Among these challenges is the misoperation of the faulted phase selection logic currently implemented in commercial protection relays. This article presents a Faulted Phase Selection (FPS) algorithm based on incremental line-to-line voltages. Considering the advantages of IEC61850 standard, the algorithm is implemented in a computer-based system using C code. The FPS operation is tested in HiL mode using an RTDS simulator. Different fault conditions are considered during the test, varying fault type, resistance, and location. Furthermore, evolving faults are also included in the tests. From the study, it is concluded that the proposed algorithm operates correctly in all analyzed scenarios.

Keywords – Centralized relay protection, Faulted phase selector algorithms, Renewable energy sources, IEC61850, Real time digital simulator, HiL

1 Introduction

The need for a more sustainable energy model to reduce the dependency on fossil fuels and greenhouse gas emissions has increased the use of Renewable Energy Sources (RES) in distribution and transmission networks.

The fault response of renewable generators based on power electronics, such as solar photovoltaics (PV) and type-IV wind turbines, differs from that of conventional synchronous generators in magnitude and fault state characteristics [1], [2]. This fact can affect the behaviour of protection algorithms currently implemented because they have been designed considering the fault characteristic of conventional synchronous generators.

Several studies show the challenges that conventional protection relays face in scenarios of high renewable penetration levels [3]–[5]. These studies usually focus on how RES affect distance protection and negative sequence components-based protection functions operation, faulted phase selection and fault direction identification.

The present paper is focused on Faulted Phase Selector (FPS) operation under a high-RES penetration level. The primary function of FPS is to classify and discriminate the phases involved during a fault. FPS is essential for correctly operating protection functions used in electric power systems, such as distance protection or fault location schemes.

Fault voltage ride-through and fast fault current injection requirements vary between countries. For example, the Spanish grid code [6] establishes that positive and negative sequence currents must be injected under unbalanced faults. By contrast, the Chilean grid code [7] suppresses the negative sequence injection in these cases.

Several studies have evaluated the impact of the grid code requirements regarding positive and negative sequence current injection under asymmetrical faults on the performance of conventional FPS algorithms. These algorithms are usually based on the phase angle relationship between sequence current components. Studies [8], [9] conclude that these FPS algorithms fail under some fault conditions, so new ones are needed.

On the other hand, the IEC 61850 standard brings new opportunities in the design of protection, control and automation systems. Among the main components of this standard are Sampled Values (SV) protocol and GOOSE messages. SV protocol transmits the digitalized voltage and current instantaneous signals measured in the electric grid to the process bus so that any device with IEC61850 protocol can subscribe to these measurements. The signal digitalization is typically carried out by Stand Alone Merging Units (SAMU). GOOSE messages are designed to satisfy the stringed requirements of high-speed protection and control applications regarding reliability and timing.

IEC 61850 offers several advantages, such as interoperability between different manufacturers' intelligent electronic devices (IED), data exchange standardization, and possibly designing a computer-assisted protection system [10].

This paper proposes a new FPS algorithm based on line-to-line incremental voltages to deal with the impact of renewable resources in the FPS operation. A computer-based system is used to implement and test the proposed FPS algorithm. The implemented system will subscribe to and publish SV and GOOSE messages generated by a real-time digital simulator (RTDS).

2 Related Work

A. Faulted Phase selection algorithms

Several FPS algorithms have been proposed in the literature [11]–[13]. They can be classified into three categories depending on the technique used to identify the faulted phase [14]:

- Power frequency components-based algorithms
- Superimposed components-based algorithms
- Transient signals-based algorithms

Traditional protection relays used in electric power system are mainly based on power frequency components to select the faulted phase. These algorithms evaluate the phase angle relationship between sequence components to discriminate the faulted phases. As an example, [15] describes an fault identification logic based on the angle relationship between negative and zero-sequence currents. Studies have shown that these algorithms often present misoperation in scenarios with high renewable penetration level because they were designed considering fault characteristics of synchronous generators.

Superimposed components technique is detailed in [16]. It evaluates the current and/or voltage variations during a disturbance, removing from transient signals its value measured one or two cycles previous to the disturbance. Superimposed components are fast and reliable methods that consider the information available during the initial transient period after fault inception. By contrast, the symmetrical components' method is slower because it uses Fourier transform.

Finally, transient signals-based techniques such as wavelet transform (WT) extracts the transient features from the original transient signal to fault detection, location and fault classification. This technique usually use a high sampling frequency [16] and are not widely implemented in commercial protection relays.

This study proposes a faulted phase selector based on superimposed line-to-line voltages to carried out the faulted phase selection in scenarios 100% renewables.

B. Using generic hardware platforms for the implementation of protection

IEC61850 standard has contributed to developing of new protection, automation and control (PAC) solutions to be applied in electric power systems. Among these solutions is the Software-defined PAC [17] based on decoupling hardware from software. This solution is an emerging technology that is gaining popularity due to advantages such as flexibility in terms of implementation and maintenance, interoperability and cost reduction compared with conventional IEDs[18].

This study implements the proposed faulted phase selector in a Desktop PC using C++ programming language.

All in all, the contribution of the present paper is twofold:

- The proposal of a new FPS algorithm based on incremental line-to-line voltages. It can be applied in scenarios with conventional synchronous generation, and with a high level of renewable penetration.
- The development of a tool that allows running a protection algorithm in a generic hardware platform, *i.e.,* a commodity PC. Thus, the code of the algorithm can either run in the commodity desktop or in a specific hardware (an IED). This allows an easy way to run the preliminary tests of the algorithm, reducing the testing time required before the final implementation.

Both contributions are tested in a hardware-in-the-loop (HiL) setup, which includes an RTDS that generates the required signals.

3 Faulted Phase Selection algorithm description

The proposed faulted phase selection algorithm (FPS) is based on the superimposed line-to-line instantaneous voltages. The algorithm structure is as follows:

- Step 1: Calculation of the superimposed line-to-line voltages ($\Delta V_{ab}(t)$, $\Delta V_{bc}(t)$, $\Delta V_{ca}(t)$)
- Step 2: Comparison of the values from Step 1 and the maximum voltage variation ($\Delta V_{ab,max}(t)$, $\Delta V_{bc,max}(t)$, $\Delta V_{ca,max}(t)$)
- Step 3: Calculation of the k-factors from the relationship between the values from Step 2
- Step 4: Perform the FPS by comparing the k-factors from Step 3 with the predefined parameters.

Following, a description of these steps is carried out.

Step 1: The superimposed line-to-line voltages are calculated using the following relationship:

$$\Delta V_{ab}(t) = \big(V_a(t) - V_b(t)\big) - \big(V_a(t-T) - V_b(t-T)\big) \quad (1)$$

$$\Delta V_{bc}(t) = \big(V_b(t) - V_c(t)\big) - \big(V_b(t-T) - V_c(t-T)\big) \quad (2)$$

$$\Delta V_{ca}(t) = \big(V_c(t) - V_a(t)\big) - \big(V_c(t-T) - V_a(t-T)\big) \quad (3)$$

where $V_a(t)$, $V_b(t)$ and $V_c(t)$ represent the instantaneous voltages values measured in the present time stamp; and $V_a(t-T)$, $V_b(t-T)$ and $V_c(t-T)$) are their corresponding values measured in the previous full cycle.

Step 2: The voltage variations calculated in the present time stamp ($\Delta V_a(t)$, $\Delta V_b(t)$ and $\Delta V_c(t)$) are compared with their corresponding maximum voltage variations, which magnitudes have been stored in memory along the time ($\Delta V_{ab,max}$, $\Delta V_{bc,max}$ and $\Delta V_{ca,max}$). If the new voltage variation exceeds the stored values, they are updated.

In the event of an evolving one, the process is also valid, but it must be slightly modified. In these cases, one cycle and a half after fault inception, the maximum voltage variations stored in memory up to this time instant are frozen and added to the voltage variations measured every time stamp to calculate the new maximum voltage variations.

Step 3: The data obtained from Step 2 are used to calculate the following factors (k_{ij}). These factors will be used to carried out the faulted phase selection.

$$k_{AB} = \frac{|\Delta V_{ab,max}|}{Max(|\Delta V_{ab,max}|, |\Delta V_{bc,max}|, |\Delta V_{ca,max}|)} \quad (4)$$

$$k_{BC} = \frac{|\Delta V_{bc,max}|}{Max(|\Delta V_{ab,max}|, |\Delta V_{bc,max}|, |\Delta V_{ca,max}|)} \quad (5)$$

$$k_{CA} = \frac{|\Delta V_{ca,max}|}{Max(|\Delta V_{ab,max}|, |\Delta V_{bc,max}|, |\Delta V_{ca,max}|)} \quad (6)$$

Step 4: To carry out the faulted phase selection, the diagram shown in **Figure 1** is used: the factors calculated in Step 3 (k_{AB}, k_{BC} and k_{CA}) are compared with a set of predefined design parameters (k_1,k_2,k_3 and k_4) to select the faulted phase. These parameters have been obtained from extensive simulations using the RTDS. In case of double line faults, the ratio between zero and positive sequence components (V_0 and V_1, respectively) is needed to distinguish between line-to-line faults and double line to ground faults.

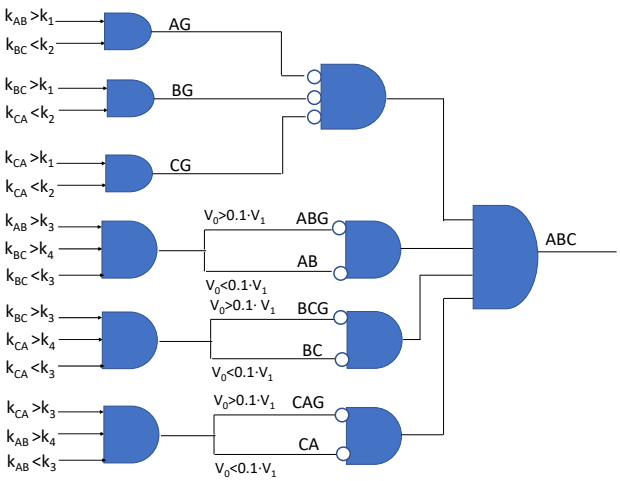

Figure 1. Faulted phase selection criterion.

4 Grid code description

RES technologies considered in this study (PV and type-IV wind turbine) are connected to the electric grid by means of power converters whose control scheme is the based on decoupled control strategy [19]. Decoupled control strategy allows to control independently the active power and the reactive power generated by the RES.

The implemented control in the power converter includes the fault voltage ride-through and fast fault current injection requirements specified in Spanish grid code [6]. **Figure 2** shows the fast fault injection requirements for the power generation modules considered during this study (generation modules with a capacity in the 100 kW to 50 MW range). As it is indicated in the figure, under unbalanced faults, the control must supply positive and negative sequence current (ΔI1 and ΔI2, respectively) proportional to the voltage dip depth (ΔU1 and ΔU2). The injection strategy used in this paper prioritizes the positive and negative sequence reactive current injection, as it is described in [20].

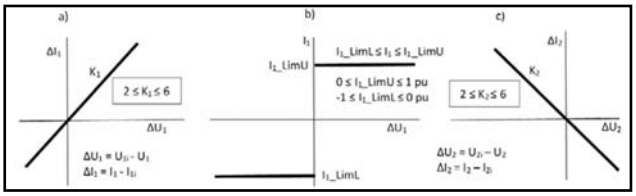

Figure 2. a) Injection/consumption of additional positive sequence reactive current (ΔI1) depending on positive sequence voltage deviation (ΔU1); b) Total reactive current (I1) injection/consumption limitation; c) Injection/ consumption of additional positive sequence reactive current (ΔI1) depending on positive sequence voltage deviation (ΔU1) [6].

5 Testing infrastructure

The distribution grid used to test the FPS algorithm is shown in **Figure 3**. In the model, the external grid is represented by a 55 kV Thevenin equivalent. This external grid is connected to a 12 kV distribution grid by means of a 55/12 kV power transformer (TR1). The study considers grounded and ungrounded grid, and two renewable technologies: a photovoltaic power plant and a type IV wind turbine. The rated power of each renewable source is 11 MW.

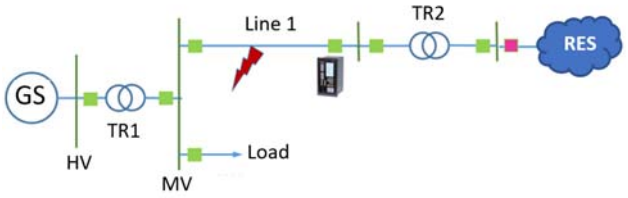

Figure 3. Benchmarking distribution grid.

To test the proposed algorithm, the following fault types are applied: Single line-to-ground faults (AG, BG and CG), line-to-line faults (AB, BC and CA), double line-to-ground faults (ABG, BCG and CAG) and three-phase faults (ABC). Furthermore, evolving faults are also applied (AG→ ABG, BG→BCG, CG→CAG, AB→ABG, BC→BCG, CA→CAG, AG→AB, BG→BC and CG→CA). Finally, two resistive faults (0 Ω and 10 Ω) are also considered.

6 Laboratory testbench description

The proposed FPS algorithm is implemented in C-code to emulate its behavior in a real protection relay. The C-code runs in a platform (a desktop PC Intel Core i5-6200U CPU, RAM 8Gb) and it was tested through the laboratory testbench described in **Figure 4**.

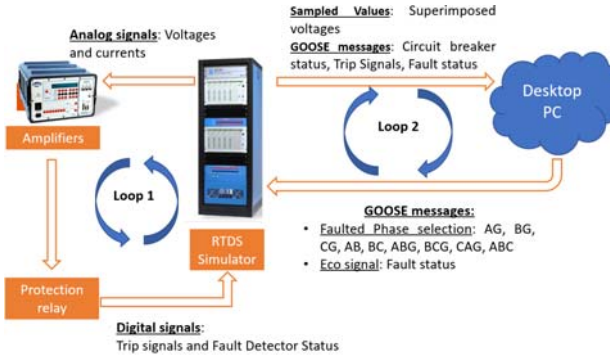

Figure 4. Laboratory testbench.

The testbench is composed by two hardware loops. The first one (Loop1) is connected to a commercial protection relay and the second one (Loop 2) is used to exchange GOOSE and Sampled Values (SV) frames between the RTDS and the Desktop PC.

By means of Loop 1, the analog current and voltages measured by instrument transformers, which are located in the line bay that is going to be protected (see **Figure 3**), are used to supply a commercial protection relay. The aim is to obtain information about the status of Trip and Fault Detector (FD) digital signals generated by the relay. These digital signals will be used as input in Loop 2.

In case of Loop 2, the RTDS publishes the superimposed line to line voltages (ΔV_{ab}, ΔV_{bc} and ΔV_{ca}) and the digital signals provided by Loop 1, according to IEC 61850-LE [21]. The platform (Desktop PC) subscribes to this information and uses it to identify the phases involved in the fault (AG, BG, CG, AB, BC, ABG, BCG, CAG or ABC).

For the FPS algorithm operation, only superimposed voltage Sampled Values are needed from simulation, but Trip Signals and the FD status from the real protection are also provided. The FD signal status is used to detect the time delays related to GOOSE messages and Sampled Values. Furthermore, FD is also used to supervise the FPS algorithm.

The algorithm distinguishes the phases involved during a fault using the previous information. Once the faulted phase selection is performed, the platform sends this information to the RTDS using GOOSE messages to show graphically the faulted phases provided by the algorithm.

7 Test results

In this section, the main results of the tests described in Section 5 are shown. These results have been selected because they are considered representative of the tests carried out during this study.

In these tests, the short circuit current is provided by the PV generation module. The figures show voltages (*VA*, *VB* and *VC*) and currents (*IA*, *IB* and *IC*) measured during the simulation under fault conditions. Furthermore, the GOOSE messages published by Desktop PC with the faulted phase information are represented by the digital signals GOOSE_AG, GOOSE_BG, etc.

Figure 5. shows an example of the FPS's behavior when an evolving fault AG→AB is applied. As can be seen in the figure, when the AG fault is applied, the fault detector signal digital (FD) is activated. Once FD is activated, the proposed algorithm identifies the fault type as AG fault and therefore, "GOOSE_AG" digital signal is activated. After 260 ms, the fault evolves to AB fault. When the evolving fault is detected, "GOOSE_AB" signal is activated. Therefore, the algorithm not only correctly detects the initial fault but also how it evolves during the entire time that the fault lasts, solving problems detected in other commercial algorithms.

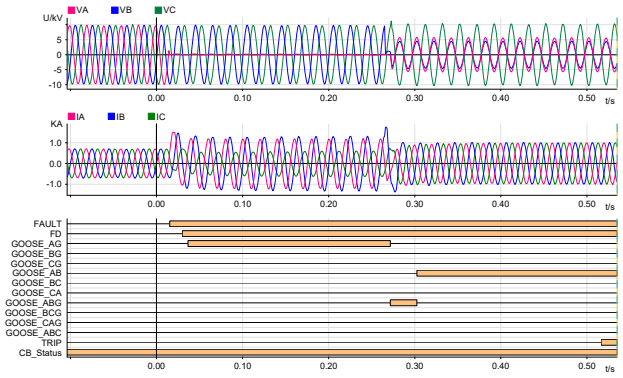

Figure 5. Faulted phase selector when evolving fault AG→AB is applied.

Figure 6 shows the FPS's behavior when a CA fault is applied. In this case, when the fault is detected, "GOOSE_CA" message is activated correctly indicating the type of fault simulated.

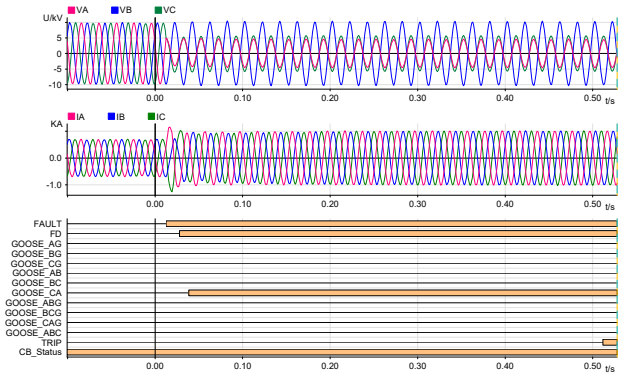

Figure 6. Faulted phase selector when CA fault is applied.

8 Conclusions

In this paper was demonstrated that the IEC 61850 standard brings new opportunities in the design of protection, control and automation systems. SV subscription was used to obtain the voltage and current instantaneous signals measured in the electric grid and GOOSE messages were used to evaluate the behaviour of the developed implementation satisfying the stringed requirements of high-speed protection and control applications regarding reliability and timing.

A new faulted phase selection algorithm based on incremental line-to-line voltages is developed and tested in a benchmarking distribution grid.

To emulate its behaviour in a commercial protection relay, it was programmed in C++ language and run on a Desktop PC.

From the conducted test, it is concluded that the developed algorithm identifies the faulted phases for all fault types in grounded and ungrounded distribution systems.

9 Acknowledgment

This work was supported in by the FLEXIGRID project from European Union's Horizon 2020 research and innovation programme under grant agreement No 864579. This paper reflects the FLEXIGRID consortium view, and European Commission is not responsible for any use that may be made of the information it contains.

10 References

[1] J. Jia, G. Yang, and A. H. Nielsen, "Investigation of grid-connected voltage source converter performance under unbalanced faults," in *2016 IEEE PES Asia-Pacific Power and Energy Engineering Conference (APPEEC)*, 2016, pp. 609–613. doi: 10.1109/APPEEC.2016.7779576.

[2] S. Impram, S. V. Nese, and B. Oral, "Challenges of renewable energy penetration on power system flexibility: A survey," *Energy Strategy Reviews*, vol. 31, p. 100539, 2020, doi: https://doi.org/10.1016/j.esr.2020.100539.

[3] Y. Fang *et al.*, "Impact of Inverter-Interfaced Renewable Energy Generators on Distance Protection and an Improved Scheme," *IEEE Transactions on Industrial Electronics*, vol. 66, no. 9, pp. 7078–7088, 2019, doi: 10.1109/TIE.2018.2873521.

[4] Power System Relay and Control Committee (Subcommittee C)– System Protection Working Group C32), "Protection Challenges and Practices for Interconnecting Inverter Based Resources to Utility Transmission Systems," Report No. PES-TR-81, IEEE, New York, Jul. 2020.

[5] O. Adeosun *et al.*, "Effect Of Inverter-Interfaced Distributed Generation On Negative Sequence Directional Element Using Typhoon Real-Time Hardware In The Loop (HIL)," in *2021 IEEE Applied Power Electronics Conference and Exposition (APEC)*, 2021, pp. 2097–2104. doi: 10.1109/APEC42165.2021.9487056.

[6] Ministerio para la Transición Ecológica y el Reto Demográfico, *Orden TED/749/2020, de 16 de julio, por la que se establecen los requisitos técnicos para la conexión a la red necesarios para la implementación de los códigos de red de conexión*, vol. BOE-A-2020-8965. 2020, pp. 62406–62458. [Online]. Available: https://www.boe.es/eli/es/o/2020/07/16/ted749

[7] NT SyCS – Comision Nacional de Energia, "Norma Técnica de seguridad y calidad del servicio," 2020. [Online]. Available: https://www.cne.cl/wp-content/uploads/2020/09/NTSyCS-Sept20.pdf

[8] A. Haddadi *et al.*, "Impact of Inverter Based Resources on System Protection," *Energies*, vol. 14, no. 4, 2021, doi: 10.3390/en14041050.

[9] S. Paladhi and A. K. Pradhan, "Adaptive Distance Protection for Lines Connecting Converter-Interfaced Renewable Plants," *IEEE Journal of Emerging and Selected Topics in Power Electronics*, vol. 9, no. 6, pp. 7088–7098, 2021, doi: 10.1109/JESTPE.2020.3000276.

[10] F. A. F. Suarez and E. Ragaini, "IEC61850-based protection system for MV/LV substations," in *2017 IEEE Workshop on Power Electronics and Power Quality Applications (PEPQA)*, 2017, pp. 1–5. doi: 10.1109/PEPQA.2017.7981690.

[11] D. Costello and K. Zimmerman, "Determining the faulted phase," in *2010 63rd Annual Conference for Protective Relay Engineers*, Mar. 2010, pp. 1–20. doi: 10.1109/CPRE.2010.5469523.

[12] R. El-Sehiemy *et al.*, "Critical aspects on wavelet transforms based fault identification procedures in HV transmission line," *IET Generation Transmission & Distribution*, vol. 10, pp. 508–517, Feb. 2016, doi: 10.1049/IET-GTD.2015.0899.

[13] K. Opoku, S. Pokharel, and A. Dimitrovski, "Superimposed Sequence Components for Microgrid Protection: A Review," in *2022 IEEE Texas Power and Energy Conference (TPEC)*, College Station, TX, USA, Feb. 2022, pp. 1–6. doi: 10.1109/TPEC54980.2022.9750756.

[14] X. Dong, W. Kong, and T. Cui, "Fault Classification and Faulted-Phase Selection Based on the Initial Current Traveling Wave," *IEEE Transactions on Power Delivery*, vol. 24, no. 2, pp. 552–559, Apr. 2009, doi: 10.1109/TPWRD.2008.921144.

[15] J. C. Quispe and E. Orduña, "Transmission line protection challenges influenced by inverter-based resources: a review," *Protection and Control of Modern Power Systems*, vol. 7, no. 1, p. 28, Jul. 2022, doi: 10.1186/s41601-022-00249-8.

[16] L. S. Azuara Grande, R. Granizo, and S. Arnaltes, "Wavelet Analysis to Detect Ground Faults in Electrical Power Systems with Full Penetration of Converter Interface Generation," *Electronics*, vol. 12, no. 5, 2023, doi: 10.3390/electronics12051085.

[17] D. Samara-Rubio *et al.*, "Virtual protection relay: A paradigm shift in power system protection." [Online]. Available: https://www.intel.com/content/www/us/en/energy/resources/virtual-production-relay-whitepaper.html

[18] Marco Nunes, "Substation Protection and Control virtualization revolution," presented at the Protection, Automation and Control World (PACWORLD). [Online]. Available: https://www.pacw.org/substation-protection-and-control-virtualization-revolution

[19] A. Egea-Alvarez *et al.*, "Advanced Vector Control for Voltage Source Converters Connected to Weak Grids," *IEEE Transactions on Power Systems*, vol. 30, no. 6, pp. 3072–3081, Nov. 2015, doi: 10.1109/TPWRS.2014.2384596.

[20] M. T. Villén *et al.*, "Influence of Negative Sequence Injection Strategies on Faulted Phase Selector Performance," *Energies*, vol. 15, no. 16, 2022, doi: 10.3390/en15166018.

[21] UCA International Users Group, "IEC 61850-9-2LE (light edition) Implementation Guideline for Digital

Interface to Instrument Transformers using IEC 61850-9-2,." [Online]. Available: www.ucainternational.org